Journal of
APPLIED PACKAGING RESEARCH

RESEARCH ARTICLE

Experimental Verification on the Effectiveness of Random Vibration Testing with Controlling Acceleration and Velocity Kurtosis

Daichi Nakai*
Sankyu Inc.

Katsuhiko Saito
Transport Packaging Laboratory,
Kobe University

ABSTRACT

Random vibration tests for packages are conducted to confirm the safety of these packages during shipping. In our previous study, a method of generating the random vibration controlling the power spectral density and kurtosis of acceleration and the kurtosis of velocity was proposed. The aim of the present study is to verify the effectiveness of the proposed method. Three vibrations were generated in this study and compared with the real vibration, which replicates the truck bed. In the first case, control of the acceleration and velocity kurtosis was neglected. In the second case, the vibration controlling the acceleration kurtosis was considered. The third case corresponded to the vibration controlling both the acceleration and velocity kurtosis generated by the proposed method. In the present study, an aluminum plate simulating the product was fixed to a table for evaluating the vibrations. The natural frequency of the plate was varied by varying the mass of the weight placed on the plate. The relative displacement of the plate was calculated from the difference between the readings of two laser displacement meters. The vibrations were evaluated via the root mean square, kurtosis, and skewness of the relative displacements of the plate. Kurtosis and skewness of the relative displacement of the proposed method were similar to those of the real vibration. However, the kurtosis and skewness of the other generated vibrations were far from those of the real vibration. Results provided experimental verification that the kurtosis of velocity is an important factor for random vibration tests.

KEY WORDS

Vibration Test, Acceleration Kurtosis, Velocity Kurtosis, Displacement Response, non-Gaussian Distribution

***Daichi Nakai**
Corresponding Author
d.nakai@sankyu.co.jp

1. INTRODUCTION

One of the purposes of packaging is to protect products from various physical hazards during distribution. Vibration is one of the most common physical hazards. Continuous external forces applied over a long period of time like vibration can destroy the product. Especially, resonance causes great damage to the product. The aim of random vibration tests for packaging is to confirm the safety of these packages from the vibration during distribution. However, the vibrations occurring in the traditional random vibration tests differ from those of the real vibrations on the truck bed [1], [2]. These differences stem from the time compression and shock-like events. Time compression can shorten the testing time by increasing the intensity of the simulation based on Basquin's law. The shock-like events, which focused on in this study, caused by road roughness, speed bumps, cracks, potholes, and metal joints. The traditional random vibration test method is unable to reproduce these shock-like events. Therefore, improving the input vibration during the vibration test is important.

The root mean square (RMS) of acceleration and power spectral density of acceleration (PSD) are used as the factors for generating random vibrations via the traditional method. The probability density of acceleration levels during a traditional vibration test is a Gaussian distribution and its kurtosis of acceleration K_a is three. However, the probability density of acceleration levels measured on a truck bed is a non-Gaussian distribution and its K_a is generally higher than three (leptokurtic) [3] - [5]. Therefore, many studies have focused on the probability density of acceleration levels and K_a during a random vibration test.

The proposed methods for improving the random vibration tests are broadly divided into two types namely, stationary and non-stationary methods.

The stationary methods can be used to transform the signal of the random vibration tests with K_a as a target. Winterstein proposes a method of generating random vibration with arbitrary K_a by distorting a Gaussian vibration using a Hermite polynomial [6]. Hosoyama et al. proposed a method for generating random vibration with arbitrary K_a by controlling the phases of a vibration [7]. The flaw of the stationary methods is that reproduction of the fluctuation in the RMS level, with period (typically) of >1 s, is impossible [8]. Hence, the probability density of the moving RMS generated by a stationary method is different from that of a real vibration.

The non-stationary methods allow easy combination of the several Gaussian vibration signals with different intensities [9] - [15]. One segment is described by a Gaussian distribution, but the entire vibration is described by a non-Gaussian distribution. The advantage of the non-stationary methods is that the probability density of the moving RMS is (in general) similar to that of a real vibration. However, the drawback of these methods is that K_a is often different from K_a of the real vibration because such methods indirectly target K_a.

The above-mentioned previous studies focused on the probability density of acceleration levels and statistical values of acceleration such as RMS, kurtosis, and a crest factor. We also consider the statistical values of velocity, which are calculated via integration of the acceleration. Moreover, we propose a method of generating the vibration controlling both the kurtosis of acceleration K_a and kurtosis of acceleration K_v [16]. We compare the generated vibrations with the real vibration using a Single Degree of Freedom (SDOF) model. The vibration with the same value of K_a as the real vibration with the vibration is compared with the vibration where K_a and K_v are both the same as those of the real vibration. Through this comparison, a significant improvement is confirmed, especially for the low-frequency domain. One aim of the proposed

method is to clarify (via experiments) the effect of K_v on product damage, because all the results of the last study are derived from numerical simulations [17].

The purpose of this study is to compare the generated vibrations with a real vibration by performing actual vibration tests and to clarify the effect of K_v on product damage through these tests. Three kinds of synthesized vibrations are considered in this study. The first is the vibration where bothK_a and K_v are three (Traditional method). The second is the vibration where K_a is the same as that of the real vibration and K_v is smaller than that of the real vibration (Previous study method). In this study, the method proposed by Hosoyama was used as the previous study method. The third is the vibration where both K_a and K_v are the same as those of the real vibration (Proposed method).

To compare the vibrations, an evaluation method is needed. Griffiths et al. proposed a device for estimating the scuffing damage and compared several generated vibrations with a real vibration [18]. However, the comparison was based on the magnitude of the scuffing damage and the natural frequencies of the products are neglected. Dunno evaluated generated vibrations by the damage to electrical products. This evaluation is practical but it is difficult to interpret the results in detail because the shapes of the products are complex [19]. Hosoyama et al. calculated the absolute acceleration response based on a SDOF model, and evaluated the cushion performance of vibration tests using the RMS and kurtosis of the acceleration response [20]. The absolute acceleration response refers to the vibration applied to the products through the cushion material. In this study, we focused on the RMS and kurtosis of the response, as well as Hosoyama's study. A relative response displacement was used rather than the absolute response acceleration. This displacement represents the difference between the absolute displacement of the product and the absolute displacement of the vibration table. The relative response displacement is proportional to the strain of the product, and is therefore considered the most representation of the product damage.

In this study, the RMS, kurtosis, and skewness of the relative displacements associated with the aluminum plate simulating the product during the vibration tests were calculated. The mass of the weight put on the plate was varied in order to change the natural frequencies of the plate. We compared vibrations generated by the traditional method, previous study method, and proposed method with the real vibration. The results revealed that, for various natural frequencies, the proposed method is more effective than the previous study method.

2. EXPERIMENTAL METHOD

2.1. Transportation test

The vertical acceleration from the truck bed was used as the real vibration. An accelerometer (Shinyei Technology Co., LTD.) was fixed in the rear center of the truck bed and to collect the vertical vibration from the road surface. Fig. 1(a) shows the truck used in this study. The suspension of the truck was leaf-ride and the maximum load of the truck is 350 kg. There was no load on the truck bed. Fig. 1(b) shows the accelerometer on the truck bed. The accelerometer sampling frequency was 4,000 Hz. Low Pass Filter was not set. Level trigger or time trigger was not set, and all acceleration data measured during driving were recorded.

The duration of the real vibration is 80 s. Fig. 2 shows the road the truck ran during transportation test. The road is paved, but the road roughness is not good compared to typical roads in Japan.

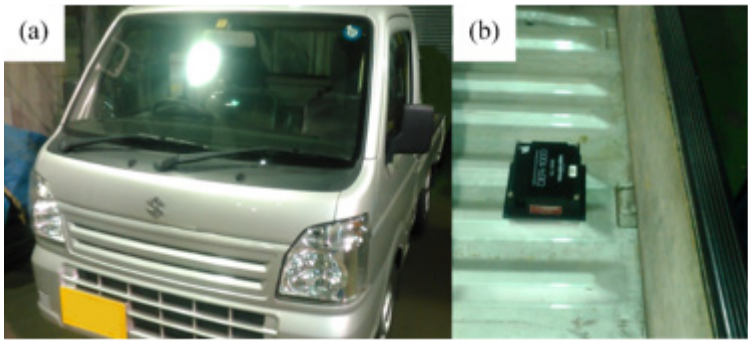

Fig. 1 Transportation test for recording acceleration (a) truck (b) truck bed and accelerometer.

Fig. 2 The road the truck ran during the transportation test.

2.2 Method for generating random vibration

The method for generating random vibrations is governed by the following expression:

$$a(t) = \sum_{k=1}^{L} A_k \cos\left(2\pi k \Delta f t + \phi_k\right), (1)$$

where, L, A_k, Δf, and ϕ_k are the number of frequency components, kth amplitude, frequency resolution, and kth phase angle, respectively. The kth amplitude is determined from:

$$A_k = \sqrt{2\Delta f P_a(k\Delta f)}, (2)$$

where, P_a $(k\Delta f)$ is a PSD. In the traditional method, ϕ_k denotes a random number ranging from 0 to 2π.

Hosoyama et al. proposed a method for using phase angles to approximate the kurtosis and probability density of acceleration (Previous study method) [7]. In a previous study method, the kth phase angle ϕ_k was given as follows:

$$\phi_k = \phi_{k-1} + 2\pi\Delta f t_{gr}(k\Delta f), (3)$$

where, t_{gr} $(k\Delta f)$ is a group-delay time. In a previous study method, t_{gr} $(k\Delta f)$ was taken as a random number with an average value m and a standard deviation denoted by σ. Moreover, m is related to the phase at which the maximum acceleration occurs, and σ is related to the envelope curve of the vibration. As σ decreases, the curve becomes

sharper, and K_a becomes higher. As σ increases, the curve becomes duller, and K_a converges to 3 (gaussian distribution).

We have shown that the σ and Δf values affect the shape of the envelop curve [16]. Δf is related to the period of the envelop curve T_d and the relationship between Δf and T_d is given as follows:

$$T_d = \frac{1}{\Delta f} \quad (4)$$

The ratio K_v/K_a decreases with decreasing T_d and converges to one with increasing T_d. In this study, T_d is 1 s as in the case of a previous study method and T_d is 10 s in the case of proposed method. Through the proposed method, we generated vibration in K_a and K_v were the same as those of the real vibration.

The duration of the real vibration is 80 second, and hence the duration of the generated vibrations is also 80 second.

2.3 Vibration test

Vibration tests were performed by A30/EM3HM and K2 controller (IMV CORPORATION). The input acceleration waveforms were resampled to 200 Hz because the maximum length of a reference waveform is 16,000 points. Resampling causes aliasing and may affect the vibration results [21]. However, the frequency components of the input acceleration in this study are mainly below 30 Hz, resampling is not expected to have a significant effect on the results. For one test condition, the vibration (duration: 80 s) was repeated four times. Furthermore, the acceleration during the tests was measured using a piezoelectric charge accelerometer type 4383 (Brüel & Kjær) and the sampling frequency was 1,000 Hz.

Figure 3 shows a schematic of the device for evaluation. The unit of dimension shown in Fig. 3 is millimeter. The general structure (ss400, JIS) of the device was fabricated from rolled steel. The four corners of the device shown in Fig. 3 were fixed to the vibration table using four hexagon head bolts (M10).

An aluminum plate (thickness: 2 mm) fabricated from aluminum alloy (A5052-O) was positioned at the center of the device with both ends fixed (Fig. 3 (b)). Fig. 4 shows the dimensions (in mm) of the plate.

Two 130×30×3.2 mm holding plates with 7.0-mm-diameter bolt holes (Fig. 3 (c)) were placed on both ends of the aluminum plate. The aluminum plate and the two holding plates were fixed using twelve hexagon head bolts (M6).

A weight was placed on the center of the aluminum plate. Eight types of weight masses were considered: 1162.4 g, 964.0 g, 768.9 g, 578.6 g, 455.1 g, 383.2 g, 284.1 g, and 189.3 g. The natural frequency of the aluminum plate decreases with increasing mass of the weight.

A 50×50×3.2 mm holding plate (Fig. 3(f)) with four 7.0-mm-diameter bolt holes was placed on the opposite side of the weight across the aluminum plate.

A relative displacement was used to evaluate the damage to the aluminum plate. The relative displacement was calculated from the differences between two displacements measured by laser displacement meters ZX-LD100 (OMRON Corporation). The meters were fixed to the frames which were around the vibration table not to move by the vibrations (Fig. 5). One of the displacement meters irradiated the laser to the center of the weight and measured the displacement of the weight (d_1) during the vibration tests. The other displacement meters irradiated the laser to the table (Fig. 3(a)) and measured the displacement of the table (d_2) during the tests. d_2-d_1 is the relative displacement d. Moreover, the weight and the table are considerably more rigid than the aluminum plate, and hence the relative displacement d is considered the deformation amount of the aluminum plate.

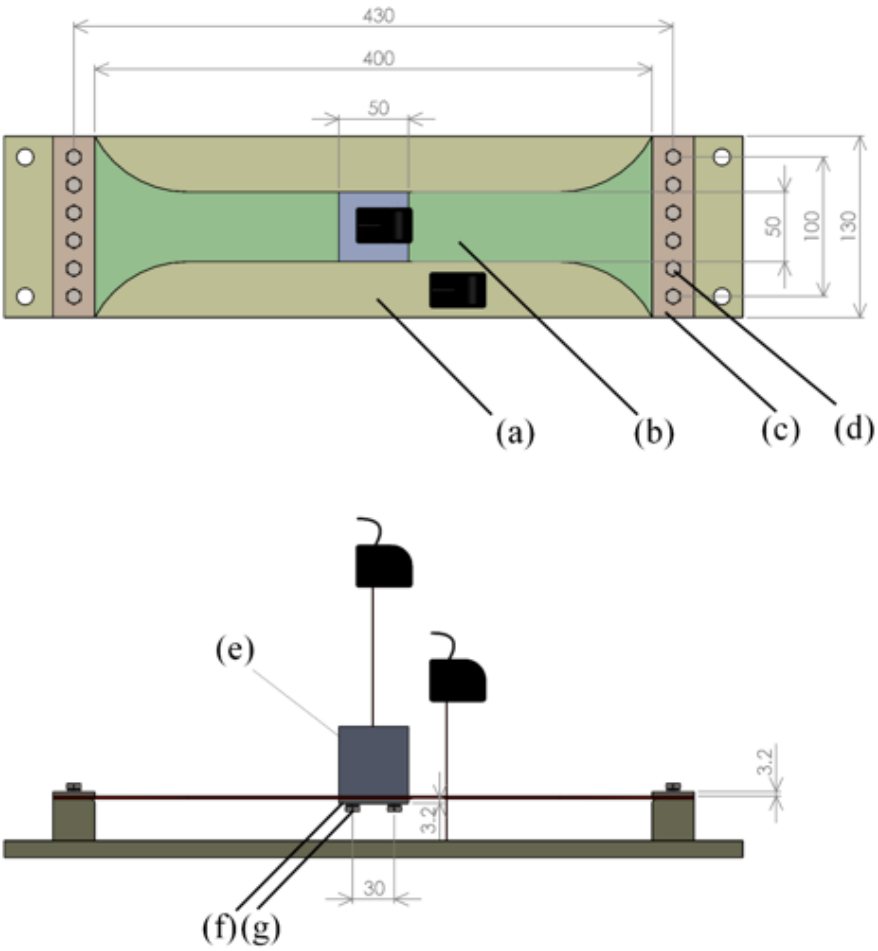

Fig. 3 Schematic showing the device for evaluation.

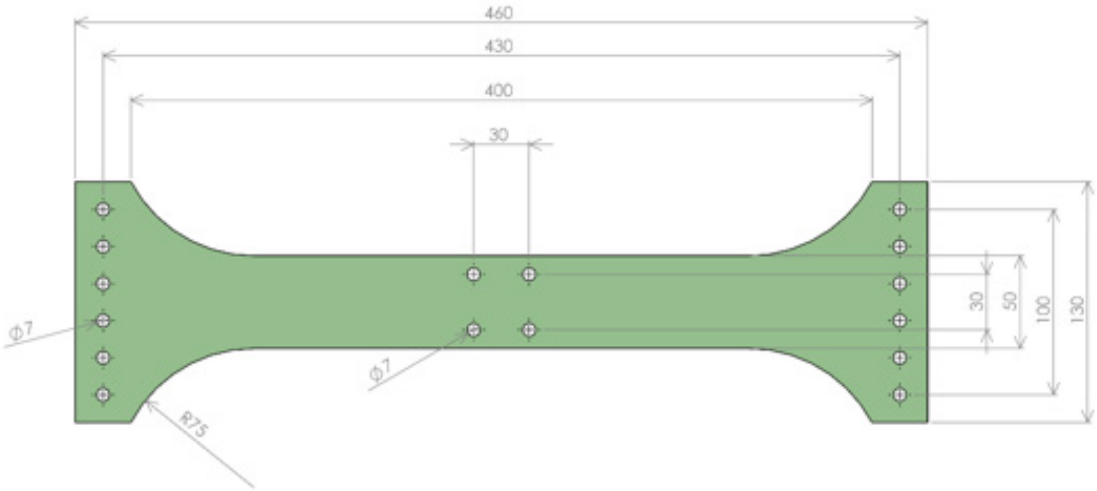

Fig. 4 Dimensions of the aluminum plate.

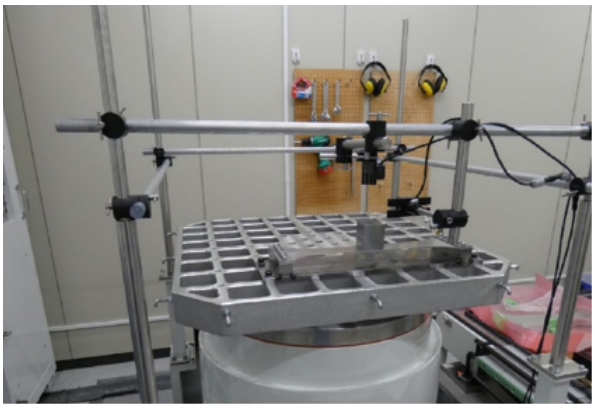

Fig. 5 A photo of the vibration test.

2.4 Frequency response function

In order to estimate the natural frequencies of the aluminum plate, a frequency response function $R(f)$ was calculated. The $R(f)$ of the aluminum plate is given as follows:

$$R(f) = \sqrt{\frac{D_1(f)}{D_2(f)}}, (5)$$

where, D_1 (f) and D_2 (f) are respectively, the Fourier transform of d_1 and the Fourier transform of d_2.

2.5 Estimation method of velocity

In this study, we calculated the time series velocity on a vibration table as follows:

$$V(f) = \frac{L(f)A(f)}{2\pi i f}, (6)$$

where, $V(f)$, $L(f)$, and $A(f)$ are respectively, the Fourier transform of velocity, the Low-cut filer, and the Fourier transform of acceleration [22]. $L(f)$ is a third-order Butterworth filter and the cutoff frequency of $L(f)$ is 0.5 Hz. The time series velocity was calculated from $V(f)$ using an inverse Fourier transform.

3. RESULTS AND DISCUSSION

3.1 Input vibrations

Figure 6 shows the time series accelerations on the vibration table. Fig. 6(a) shows the real vibration, which replicate the vibration on the truck bed. Fig. 6(b) shows the vibration generated by the traditional method, where nearly all of the acceleration values were <10 m/s^2. Fig. 6 (c) shows the vibration generated by the previous study method, where the acceleration was higher than that of the traditional method. The cycle of the envelop curve shown in Fig. 6 (c) was 1 s. Fig. 6(d) shows the vibration generated by the proposed method. The cycle of the envelop curve shown in Fig. 6 (d) was 10 s.

Figure 7 shows the probability density functions (PDF) of acceleration on the vibration table. The PDF of acceleration associated with the traditional method (Fig. 7(b)) was described by an almost Gaussian distribution. The PDFs associated with the real vibration (Fig. 6(a)), previous study method (Fig. 7(c)), and proposed method (Fig. 7 (d)) were described by non-Gaussian distributions and had quite similar shape.

Figure 8 shows time series velocities on the vibration table. The velocities were calculated from the accelerations shown in Fig. 6 using equation (6) and inverse Fourier transform. Fig. 8(a) shows the velocity of the real vibration, where high velocity values of >0.3 m/s occurred. Fig. 8(b) shows the velocity of the traditional method, where only velocity values of <0.3 m/s were observed. Fig. 8(c) shows the velocity of the previous study method. Although high acceleration values were observed, as shown in Fig. 7(c), high velocity values of >0.3 m/s were absent. Fig. 8(d) shows the velocity obtained for the proposed method. In contrast to the results obtained for the previous study method (see Fig. 8(c)), high velocity values of >0.3 m/s were observed for the proposed method.

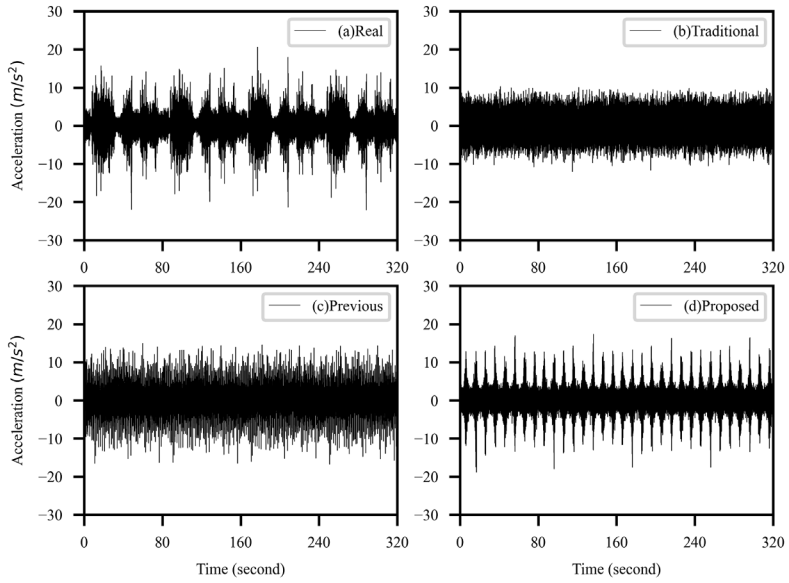

Fig. 6 Time series acceleration on the vibration table, (a) Real vibration, (b) Traditional method, (c) Previous study method, and (d) Proposed method.

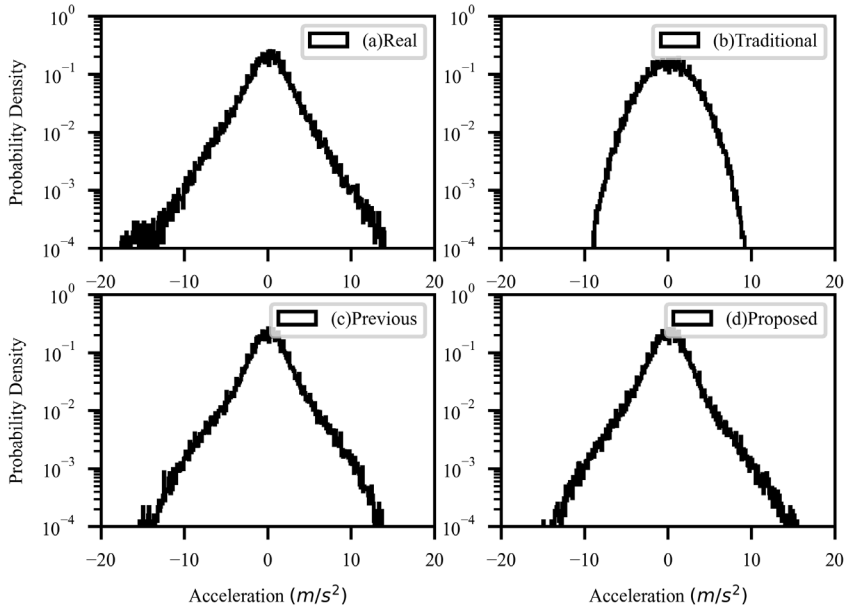

Fig. 7 Probability density function of acceleration on the vibration table, (a) Real vibration, (b) Traditional method, (c) Previous study method, and (d) Proposed method.

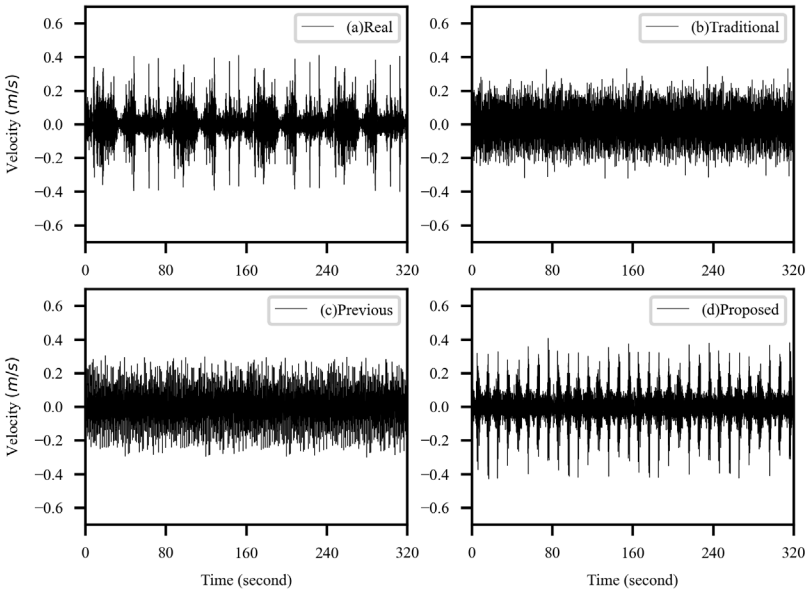

Fig. 8 Time series velocity on the vibration table, (a) Real vibration, (b) Traditional method, (c) Previous study method, and (d) Proposed method.

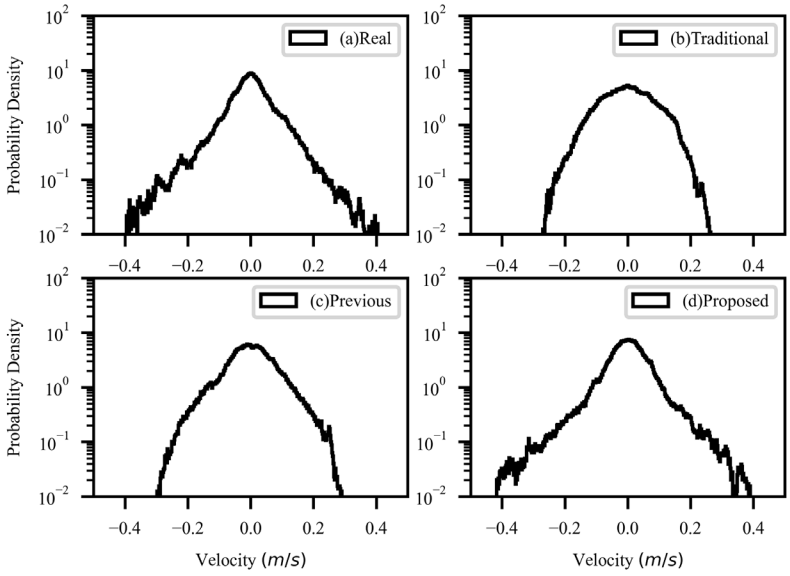

Fig. 9 Probability density function of velocity levels on the vibration table, (a) Real vibration, (b) Traditional method, (c) Previous study method, and (d) Proposed method.

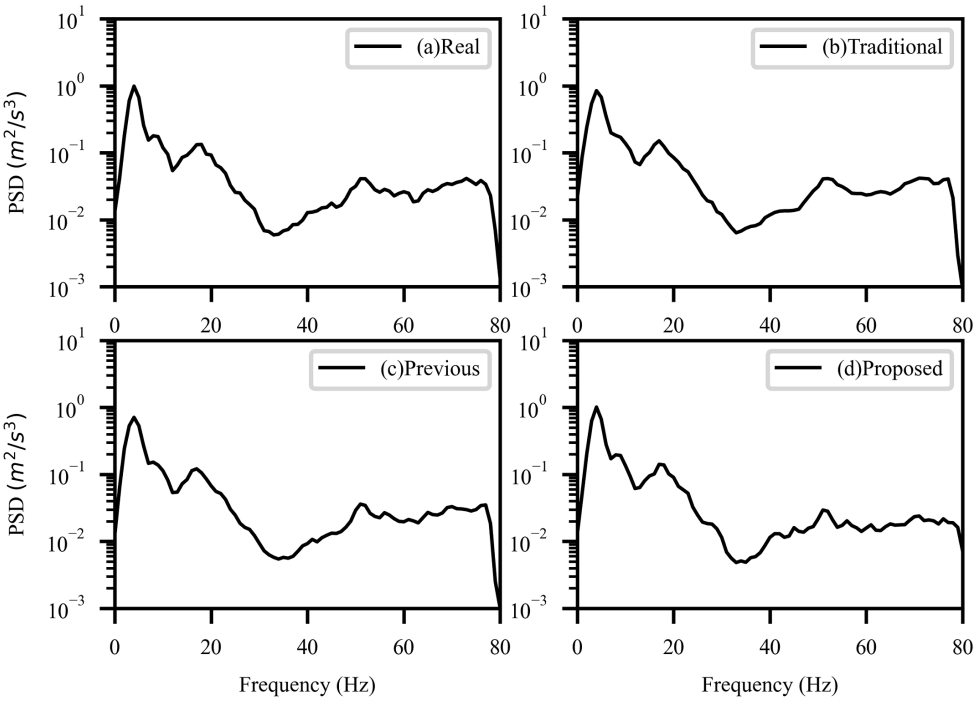

Fig. 10 Power spectral density of acceleration, (a) Real vibration, (b) Traditional method, (c) Previous study method, and (d) Proposed method.

Figure 9 shows the PDFs of velocity on the vibration table. Fig. 9(a) shows the PDF of the velocity during the real vibration. The PDF of the velocity during the traditional method (Fig. 9(b)) was described by an almost Gaussian distribution, as in the case of the density obtained for acceleration. Fig. 9(c) and Fig. 9 (d) show respectively, the probability density of velocity obtained during the previous study method and the proposed method. The probability density corresponding to acceleration of the real vibration, previous study method, and proposed method were of the same shape. However, the outliers of the density associated with the velocity during the previous study method were narrower than those of the real vibration and the proposed method. In contrast, the PDF of velocity during the real vibration and proposed method had the same shape.

Figure 10 shows PSDs of the acceleration. Fig. 10 (a), (b), (c), and (d) show respectively, the PSDs obtained for the real vibration, traditional method, previous study method, and proposed method. Due to the ability of the vibration controller, only PSDs of up to 80 Hz was controlled. Therefore, Fig. 10 shows the PSD up to 80 Hz. The results shown in Fig. 10 (a)–(d) differed only slightly. The peaks of the PSD were 4 Hz and 17 Hz.

Table 1 shows the RMS of acceleration and RMS of velocity on the vibration table. The RMS values corresponding to the accelerations of the real vibration, traditional method, previous study method, and proposed method were almost the same. Similarly, the RMS values of the velocities were almost the same.

Table 1 Acceleration RMS and Velocity RMS.

No.	Weight (g)	Acceleration RMS (m/s^2)				Velocity RMS (m/s)			
		Real	Traditional	Previous	Proposed	Real	Traditional	Previous	Proposed
1	1455.1	2.49	2.73	2.51	2.40	0.077	0.091	0.081	0.079
2	1162.4	2.53	2.53	2.51	2.45	0.076	0.081	0.080	0.079
3	964.0	2.46	2.50	2.47	2.42	0.076	0.082	0.081	0.079
4	768.9	2.47	2.49	2.47	2.41	0.076	0.082	0.080	0.079
5	578.6	2.46	2.46	2.47	2.41	0.076	0.081	0.081	0.079
6	383.2	2.45	2.47	2.47	2.39	0.076	0.081	0.081	0.079
7	284.1	2.45	2.47	2.46	2.40	0.076	0.081	0.080	0.079
8	189.3	2.46	2.46	2.47	2.41	0.076	0.081	0.080	0.079
	Average	2.47	2.51	2.48	2.41	0.076	0.083	0.080	0.079

Table 2 Acceleration kurtosis and Velocity kurtosis.

No.	Weight (g)	Acceleration Kurtosis K_a				Velocity Kurtosis K_v			
		Real	Traditional	Previous	Proposed	Real	Traditional	Previous	Proposed
1	1455.1	7.20	2.88	6.50	6.92	6.40	2.81	3.76	6.66
2	1162.4	6.51	2.97	6.33	6.64	6.44	2.79	3.70	6.70
3	964.0	6.85	2.90	6.53	6.95	6.38	2.82	3.67	6.67
4	768.9	6.97	2.95	6.56	7.08	6.44	2.81	3.68	6.78
5	578.6	7.01	2.99	6.71	7.12	6.43	2.81	3.65	6.68
6	383.2	6.94	2.89	6.58	7.02	6.43	2.82	3.64	6.71
7	284.1	6.98	2.93	6.68	6.99	6.39	2.80	3.70	6.71
8	189.3	6.92	2.89	6.61	6.92	6.47	2.80	3.67	6.65
	Average	6.92	2.92	6.56	6.95	6.42	2.81	3.68	6.70

Table 2 shows the kurtosis of acceleration K_a and the kurtosis of velocity K_v. K_a and K_v were close to three in the case of the traditional method. Hence, both the acceleration and velocity of the vibration generated by this method were described by a Gaussian distribution. Although the K_a of the previous study method was 6.56, which is considerably higher than 3, the K_v of this method was 3.68, i.e., close to 3. The K_a and K_v of the real vibration and the proposed method were quite similar. The results shown in Table 2 are consistent with the probability density of acceleration and velocity shown in Fig. 7 and Fig. 9. Despite the differences between an actual vibration test and a

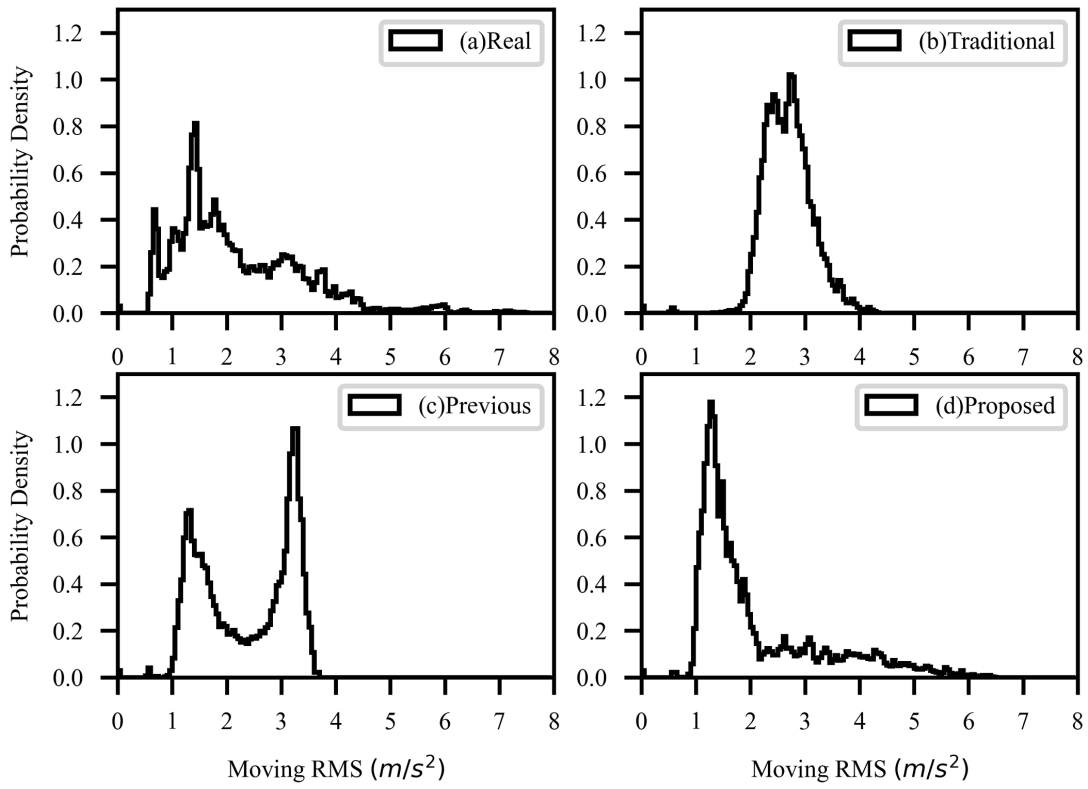

Fig. 11 Probability density function of moving acceleration RMS (window length 0.5 s), (a)Real vibration, (b) Traditional method, (c) Previous study method, and (d) Proposed method.

numerical simulation, the above results regarding input vibrations are consistent with the results of our previous study [16].

Figure 11 shows the PDF of the moving acceleration RMS. The window length of moving RMS was set to 0.5 s [23]. The probability density of the real vibration had a peak at 1.5 m/s^2 and a wide range of values (0.5 m/s^2 to 6.0 m/s^2) as shown in Fig. 11(a). The PDF of the traditional method (Fig. 11(b)) had a peak at 2.8 m/s^2 and a range of values (1.8 m/s^2 to 4.2 m/s^2), which were narrower than that of the real vibration. The PDF of the previous study method (Fig. 11(c)) had peaks at 1.5 m/s^2 and 3.3 m/s^2 and a range of values from 1.0 m/s^2 and 3.6 m/s^2. Although K_a of the previous study method was close to that of the real vibration, among the PDFs, the PDF of the moving acceleration RMS was the most different from that of the real vibration. The PDF of the proposed method (Fig. 11(d)) had a peak at 1.5 m/s^2 (range of values: 1.0 m/s^2 to 6.0 m/s^2) and was most similar to that of the real vibration.

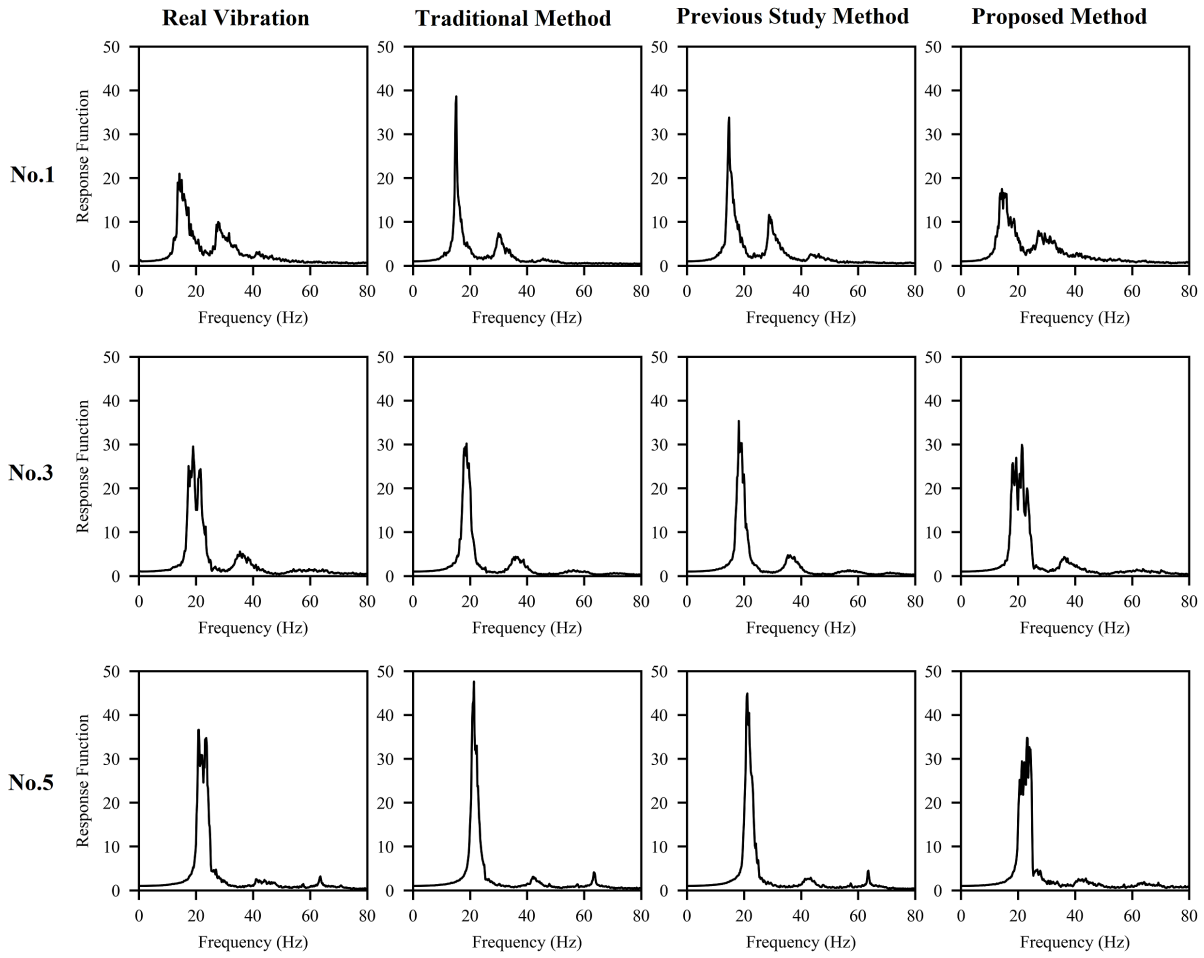

Fig. 12 Response frequency function R(f).

3.2 Aluminum plate deformation

Figure 12 shows the frequency response function $R(f)$ calculated from equation (5). "No." in Figs. 12, 13, and 14. corresponds to the "No." shown Tables 1 and 2. Nos. 1, 3, and 5 are shown in Fig. 12.

In the case of No. 1, the peaks of $R(f)$ were 15.2 Hz, 30 Hz, and 46.4 Hz. These frequencies were multiples of 15 Hz and were assumed to be the natural frequencies of the aluminum plate. The peak values of $R(f)$ remained unchanged even with changes in the input vibration.

In contrast, the mass had an effect on the peak frequency values. In the case of No. 3, the peaks of $R(f)$ were 18.8 Hz, 36.6 Hz, and 56.2 Hz. This indicated that the natural frequencies of the aluminum plate increased with decreasing mass of the weight.

The input vibration had an effect on the sharpness of the peaks obtained for $R(f)$. The $R(f)$ peaks of the traditional method and previous study method were sharper than those of the real vibration and proposed method. However, especially when the mass of the weight was heavy like No. 1, the maximum peak values of the real vibration and proposed method were lower and the peak widths were wider than those of the traditional method and previous study method.

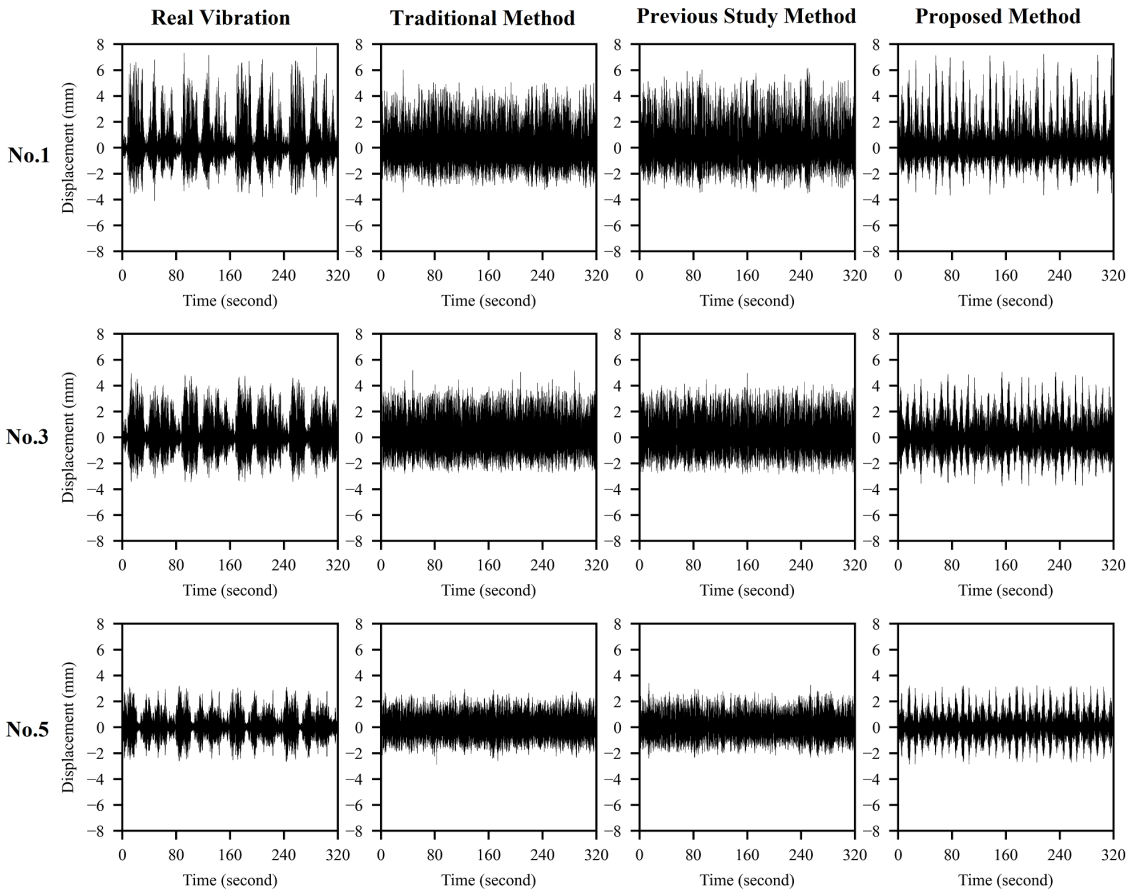

Fig. 13 Time series relative displacements of the aluminum plate.

Figure 13 shows the time series relative displacement d. When the weight was placed on the aluminum plate without vibration, d=0 mm. When the plate deformed in the direction opposing gravity, d was >0. When the weight was unloaded after the vibration test, no clear deformation of the plate could be confirmed under any test condition. The relative displacement increased with increasing mass of the weight. Regardless of the test No., the maximum displacements of the real vibration were greater than those of the traditional method.

The relative displacements in the upward direction (i.e., opposite to the direction of gravity) were greater than those in the downward direction (i.e., the direction of gravity). This vertical asymmetry was attributed to the shape of the response function. The asymmetry of the relative displacement means that the spring constant of the aluminum plate is non-constant. The natural frequencies depend on the spring constant, and fluctuations of this constant led to the dull peaks of the response function.

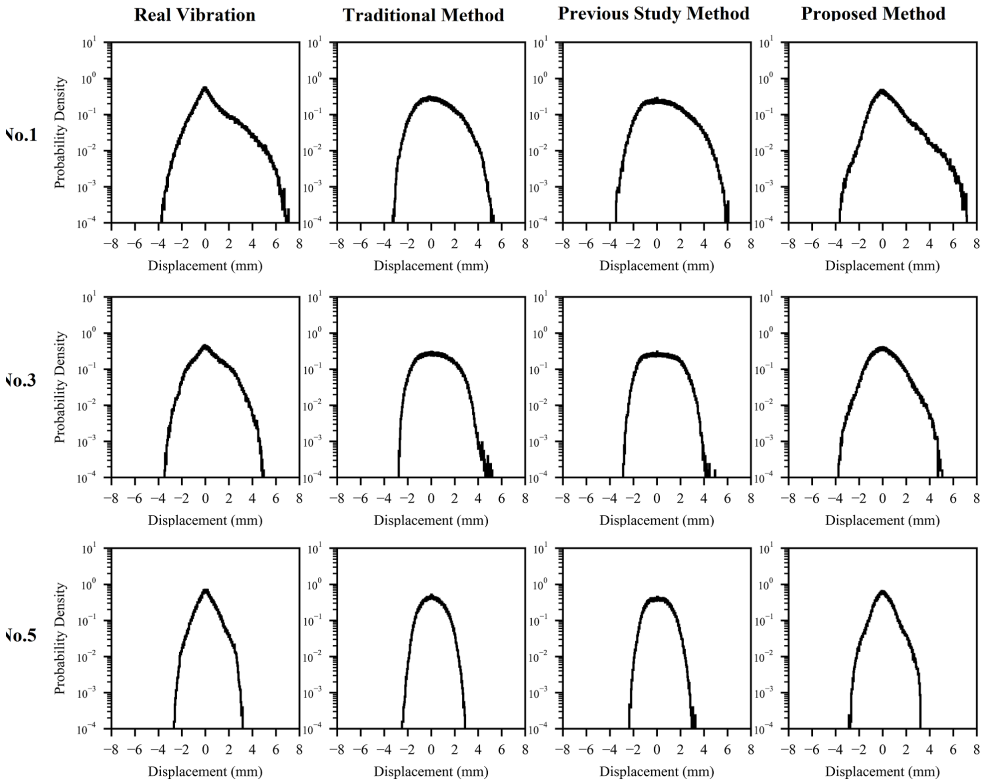

Fig. 14 Probability density function obtained for the relative displacements of the aluminum plate.

Figure 14 shows the PDFs of the relative displacement *d*. The probability densities of the real vibration and proposed method were leptokurtic. Moreover, for all test numbers, the probability densities of the proposed method were similar to those of the real vibration. In contrast, the densities of the traditional method and previous study were platykurtic and differed considerably from those of the real vibration.

Figure 15 shows the RMS values of the relative displacement *d*. The horizontal axis shows the natural frequency, where $R(f)$ is a maximum. $R(f)$ corresponds to the lowest natural frequency and the smallest experiment number. The mass of the weight and the RMS of the relative displacement decreased with increasing natural frequency. Regardless of the natural frequency, all vibrations in this study had almost the same relative displacement RMS values.

Figure 16 shows the kurtosis of the relative displacement *d*. The horizontal axis shows the natural frequency. The same tendency was observed for the traditional method and the previous study method and this tendency differed significantly from the real vibration. In most cases, these kurtosis values were smaller than three (platykurtic). In contrast, the proposed method was similar to the previous study method. The kurtosis values of the real vibration and proposed method were greater than three (leptokurtic). Although K_a and K_v of the real vibration and proposed method were greater than six, the kurtosis associated with the relative displacement of the real

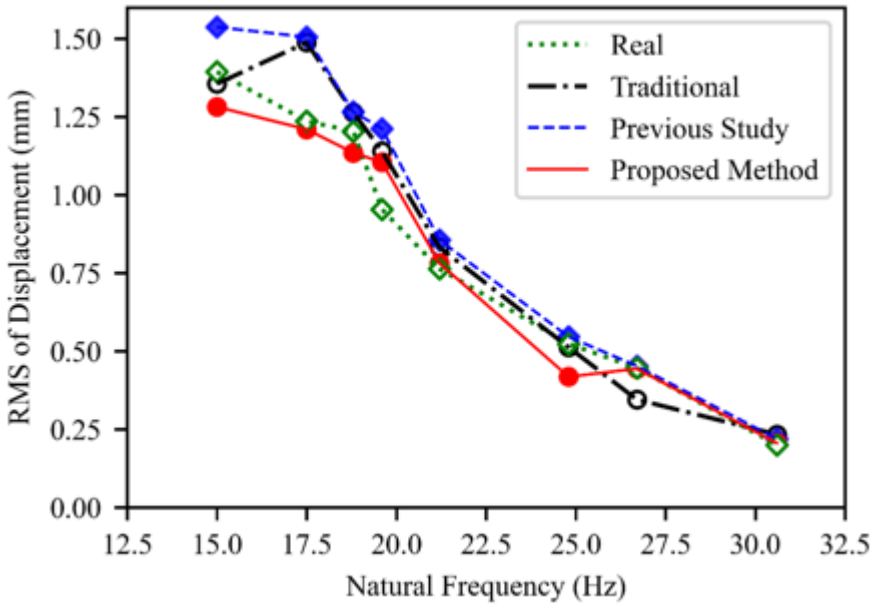

Fig. 15 Relationship between RMS of the aluminum displacement and natural frequency.

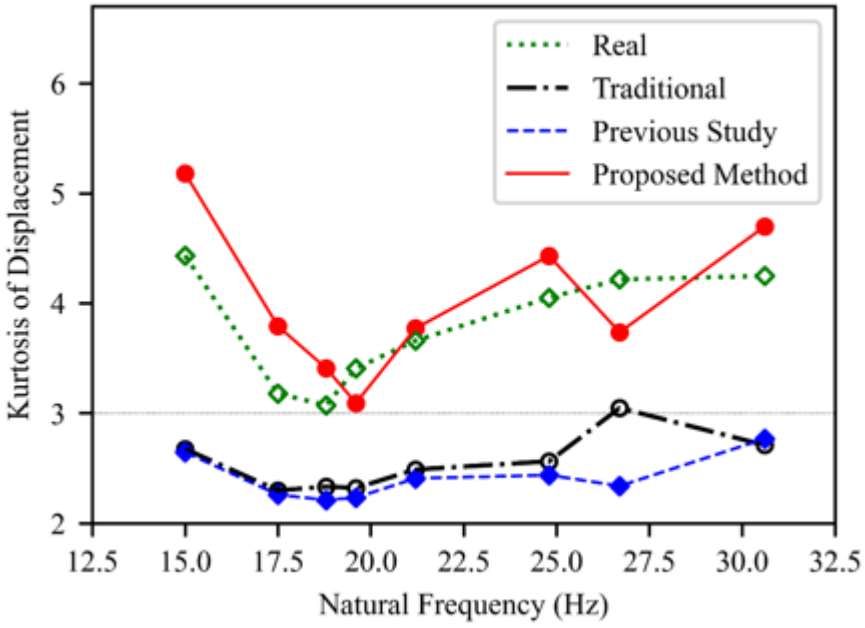

Fig. 16 Relationship between Kurtosis of the aluminum displacement and natural frequency.

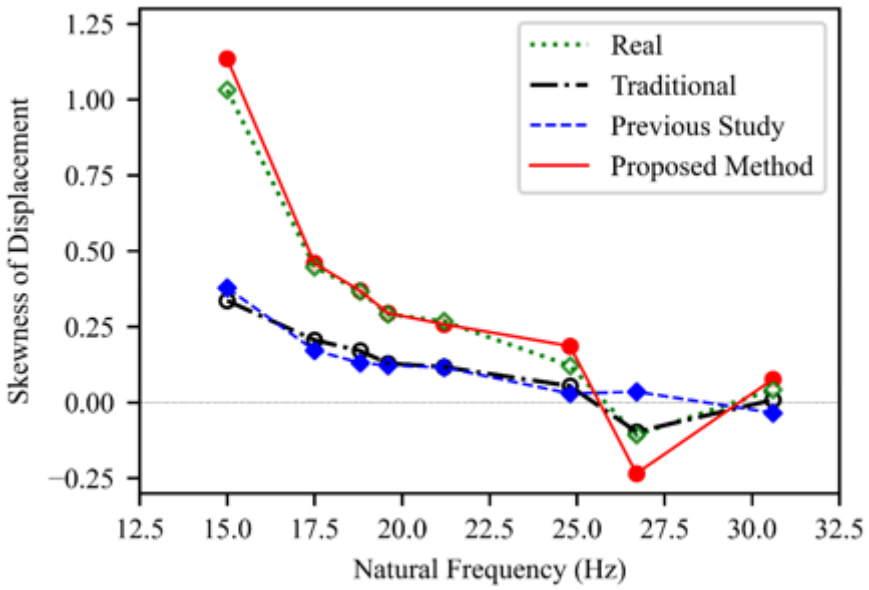

Fig. 17 Relationship between skewness of the aluminum displacement and natural frequency.

vibration and proposed method were smaller than six. The difference between the kurtosis of the input vibration and the kurtosis of the response vibration was also observed by Hosoyama et al. [20].

Figure 17 shows the skewness of the relative displacement *d*. The horizontal axis shows the natural frequency. The asymmetry increased with increasing skewness. Furthermore, the mass of the weight decreased with increasing natural frequency, whereas the skewness of the relative displacement decreased. The same tendency was observed for the traditional method and previous study method and this tendency differed significantly from the real vibration. In contrast, the proposed method was similar to the previous study method.

As described above, in the case of the traditional method and previous study method, the displacement of the aluminum plate during the vibration test was smaller than that of the real vibration. In general, the effect on Fatigue is not proportional to the amount of strain or input acceleration, but is proportional to the n-th power of the amount of strain or input acceleration (n is greater than or equal to 2) [1]. Therefore, in the case of the traditional method and previous study method, the effect of vibration on fatigue is assumed to be underestimated. This may cause underpackaging. On the other hand, in the case of the vibration test using the proposed method, the displacement of the aluminum plate is close to the real vibration, and it is assumed that the effect of vibration on fatigue is evaluated more appropriately than in the traditional method or previous study method.

3.3 Limitations

The results on kurtosis and skewness are not giving the real relationship for product-packaging system, because aluminum plate is not equal to product-packaging system in real practice. The effects of time compression on the deformation amount of the aluminum plate are not considered in this paper.

4. CONCLUSIONS

We compared the real vibration and three vibrations, which were generated based on statistical values of this vibration. For the first vibration, K_a and K_v were both three (Traditional method). The second vibration corresponded to the case where K_a was the same as that of the real vibration (Previous study method). For the third vibration, K_a and K_v were the same as those of the real vibration (Proposed method). These vibrations were evaluated via the RMS, kurtosis, and skewness associated with the relative displacements of the aluminum plate simulating the product.

The RMS associated with the relative displacement of the aluminum plate differed only slightly among the four vibrations. However, the kurtosis and skewness associated with the relative displacement of the traditional method and the previous method differed significantly from those of the real vibration. In contrast, the kurtosis and skewness associated with the relative displacement of the proposed method were similar to those of the real vibration.

From these results, it is experimentally confirmed that K_v is an important factor for random vibration tests for packaging. When vibration tests are conducted using the traditional method or previous study method, the amount of damage to the product is smaller than that of real vibration, which may cause underpackaging. On the other hand, the proposed method is more appropriate than the previous study method to evaluate the damage to the product.

In future work, we will clarify the velocity kurtosis during transportation.

REFERENCES

[1] J. Lupine, V. Rouillard and M.A. Sek, "Review paper on road vehicle vibration simulation for packaging testing purposes," Packaging Technology and Science, vol. 28, (8) pp. 657-671, 2015.

[2] W.I. Kipp, Accelerated random vibration with time-history shock, IoPP 2001 Annual Membership Meeting, San Jose (CA), USA, 2001.

[3] M.P. Kurniawan, V. Chonhenchob, S.P. Singh and S. Sittipod, "Measurement and analysis of vibration levels in two and three wheel delivery vehicles in Southeast Asia," Packaging Technology and Science, vol. 28, (9) pp. 836-850, 2015.

[4] H. Zhou and Z.W. Wang, "Measurement and analysis of vibration levels for express logistics transportation in South China," Packaging Technology and Science, vol 31, (10) pp. 665-678, 2018.

[5] P. Böröcz and S.P. Singh, "Measurement and analysis of delivery van vibration levels to simulate package testing for parcel delivery in Hungary," Packaging Technology and Science, vol 31, (5) pp. 342-352, 2018.

[6] S.R. Winterstein, "Nonlinear vibration models for extremes and fatigue," Journal of Engineering Mechanics, vol 114, (10) pp. 1772-1790, 1988.

[7] A. Hosoyama, K. Saito and T. Nakajima, "Non-Gaussian random vibrations using kurtosis," in Eighteenth IAPRI World Packaging Conference, DEStech Publications, Inc.: San Louis Obispo (CA), USA, 2012.

[8] V. Rouillard, "Quantifying the non-stationarity of vehicle vibrations with the run test," Packaging Technology and Science, vol 27, (3) pp. 203-219, 2014.

[9] V. Rouillard and M. A. Sek, "Synthesizing nonstationary, non-Gaussian random vibrations," Packaging Technology and Science, vol 23(8), pp. 423-439, 2010.

[10] V. Rouillard and M.A. Sek, "Monitoring and simulating non-stationary vibrations for package optimization," Packaging Technology and Science, vol. 13, (4) pp. 149-156, 2000.

[11] J. Singh, S.P. Singh and E. Joneson, "Measurement and analysis of US truck vibration for leaf spring and air ride suspensions, and development of tests to simulate these conditions," Packaging Technology and Science, vol. 19, (6) pp. 309-323, 2006.

[12] W.I. Kipp., "Random vibration testing of packaged-products: considerations for methodology improvement," Sixteenth IAPRI World Conference on Packaging: Bangkok, Thailand, 2008.

[13] V. Rouillard, "On the non-Gaussian nature of random vehicle vibrations," World Congress on Engineering, London, UK, 2007.

[14] K.R. Griffiths, B.J. Hicks, P.S. Keogh and D. Shires, "Wavelet analysis to decompose a vibration simulation signal to improve pre-distribution testing of packaging," Mechanical Systems and Signal Processing, vol. 76-77, pp. 780-795, 2016.

[15] H. Zhou and Z.W. Wang, "A new approach for road-vehicle vibration," Packaging Technology and Science, vol. 31, (5) pp. 246-260, 2018.

[16] D. Nakai and K. Saito, “A method for generating random vibration using acceleration kurtosis and velocity kurtosis,” Journal of Applied Packaging Research, vol. 11, (2) pp. 64-74, 2019.

[17] D. Nakai and K. Saito, “A Method for Generating Random Vibration Considering Kurtosis Response Spectrum,” Journal of Packaging Science & Technology, Japan, vol. 30, (4) pp. 261-272, 2021.

[18] K.R. Griffiths, D. Shires, W. White, P.S. Keogh, B.J, Hicks, “Correlation study using scuffing damage to investigate improved simulation techniques for packaging vibration testing,” Packaging Technology and Science, vol. 26, (7) pp. 373-383, 2013.

[19] K. Dunno, “Experimental Evaluation of Techniques Designed to Reduce Vibration Simulation Test Time,” Journal of Applied Packaging Research, Vol. 6, (2) pp. 1-10, 2014.

[20] A. Hosoyama, K. Tsuda, S. Horiguchi, “Development and validation of kurtosis response spectrum analysis for antivibration packaging design taking into consideration kurtosis,” Packaging Technology and Science, vol. 33, (2) pp. 51-64, 2020.

[21] V. Rouillard and M. Lamb, “On the effects of sampling parameters when surveying distribution vibrations,” Packaging Technology and Science, Vol. 21, (8), pp. 467-477, 2008.

[22] D. Nakai and K. Saito, “Estimation method of velocity on Truck Bed,” Twenty-second IAPRI World Packaging Online Conference, Monterrey, Mexico 2020.

[23] H. Zhou and Z.W. Wang, “Comparison study on simulation effect of improved simulation methods for packaging random vibration test,” Packaging Technology and Science, vol. 32, (3) pp. 119-131, 2018.